Marine Geology xxx (2009) xxx–xxx

Contents lists available at ScienceDirect

Marine Geology

journal homepage: www.elsevier.com/locate/margeo

Sediment accumulation patterns and fine-scale strata formation on the Waiapu River shelf, New Zealand

Tara A. Kniskern [a,*], Steven A. Kuehl [a], Courtney K. Harris [a], Lionel Carter [b]

[a] Virginia Institute of Marine Science, College of William and Mary, P.O. Box 1346, Gloucester Point, VA 23062, USA
[b] Antarctic Research Centre, Victoria University of Wellington, P.O. Box 600, Wellington 6001, New Zealand

ARTICLE INFO

Article history:
Accepted 16 December 2008
Available online xxxx

Keywords:
continental shelf
sedimentation
^{210}Pb
^{7}Be
New Zealand
gravity-flows

ABSTRACT

Multiple sediment transport and reworking processes influence fine, cm-scale strata formation and long-term accumulation on the Waiapu River shelf, New Zealand. Gravity cores collected during two cruises, in August 2003 and May 2004, were analyzed using ^{7}Be and ^{210}Pb geochronologies, bulk carbon, δ^{13}C, X-radiographs, and grain-size to investigate sediment mixing and accumulation patterns. The presence of ^{7}Be on the inner- and mid-shelf regions (<~80m) indicated recent (within the last 4–5 months) deposition of fluvial muds, whereas the distribution of excess ^{210}Pb accumulation rates revealed that the middle to outer shelf (50–130 m) acted as fine sediment repositories on longer time scales. Excess ^{210}Pb accumulation rates were high, with an area weighted average of 1.1±0.1 cm/yr and ranging between 0.2 and 3.5 cm/yr, yet were localized such that only an estimated ~23% (ranging between 17 and 38%) of the fluvial load was retained on the shelf between 40 and 200 m depths over the last 80 to 100 yr. Sediments not retained on the shelf were either transported to deeper waters or along the shelf beyond the sampling area.

Several cores collected from the high sediment accumulation zone on the middle to outer shelf exhibited non-steady state excess ^{210}Pb profiles, suggesting that multiple transport processes influenced fine-scale strata formation. Layers of low excess ^{210}Pb activity and predominantly terrestrial δ^{13}C and C/N values were likely formed during floods, when sediments were rapidly deposited and buried on the shelf. These event layers were sufficiently thick (up to ~20 cm), such that all or a portion of the initial flood layer immediately transited through the surface mixing layer, ensuring preservation in the sediment record. Sediments inter-bedded with these event layers reflected a relatively marine source indicating either that they were not deposited rapidly or were significantly bioturbated. A gradient of physical and biological mixing signatures, extending radially from the Waiapu River mouth, suggested that high background accumulation rates and flood deposits negatively impacted the preservation of biological structures and enhanced preservation of event-produced beds.

1. Introduction

Recent research has focused on narrow, steep continental shelves along collision margins because fluvial dispersal on these shelves accounts for over half of the world's terrigenous input (Milliman et al., 1999; Farnsworth and Milliman, 2003). Small rivers on collision margins are characterized by mountainous catchments composed of highly erodible materials contributing to some of the earth's highest sediment yields (Griffiths and Glasby, 1985; Milliman et al., 1999, Hicks et al., 2004). Sediment delivery tends to be episodic, with floods delivering a significant fraction of a small river's annual load (Milliman and Syvitski, 1992; Farnsworth and Milliman, 2003; Hicks et al., 2004) often during energetic oceanic conditions (Wheatcroft and Sommerfield, 2005).

Multiple transport mechanisms disperse flood sediments, influencing fine-scale strata formation, and accumulation patterns on the shelf (Mulder and Syvitski, 1995; Morehead and Syvitski, 1999; Kineke et al., 2000, Friedrichs and Wright, 2004; Ma et al., 2008). Although fluvial sediments are typically dispersed in buoyant plumes, suspended sediment concentrations in these small rivers can exceed the threshold for negatively buoyant, gravity-driven, hyperpycnal plumes (Mulder and Syvitski, 1995; Hicks et al., 2004). Additionally, when sediment flux convergence forms highly turbid benthic layers, sediments may be transported across the shelf bathymetry within gravity-driven flows (Ogston et al., 2000; Traykovski et al., 2000; Wright et al., 2001, 2002; Friedrichs and Wright, 2004; Harris et al., 2005; Ma et al., 2008). To create sufficient turbulence to maintain a gravity flow requires energetic waves or currents or a shelf slope >0.01 (Friedrichs and Wright, 2004, Wright and Friedrichs, 2006). Few studies, however, have observed gravity-driven flows on shelves (Ogston et al., 2000; Traykovski et al., 2000) or linked this transport

* Corresponding author. Tel.: +1 804 684 7762; fax: +1 804 684 7250.
E-mail addresses: knista@vims.edu (T.A. Kniskern), kuehl@vims.edu (S.A. Kuehl), ckharris@vims.edu (C.K. Harris), Lionel.Carter@vuw.ac.nz (L. Carter).

0025-3227/$ – see front matter © 2008 Elsevier B.V. All rights reserved.
doi:10.1016/j.margeo.2008.12.003

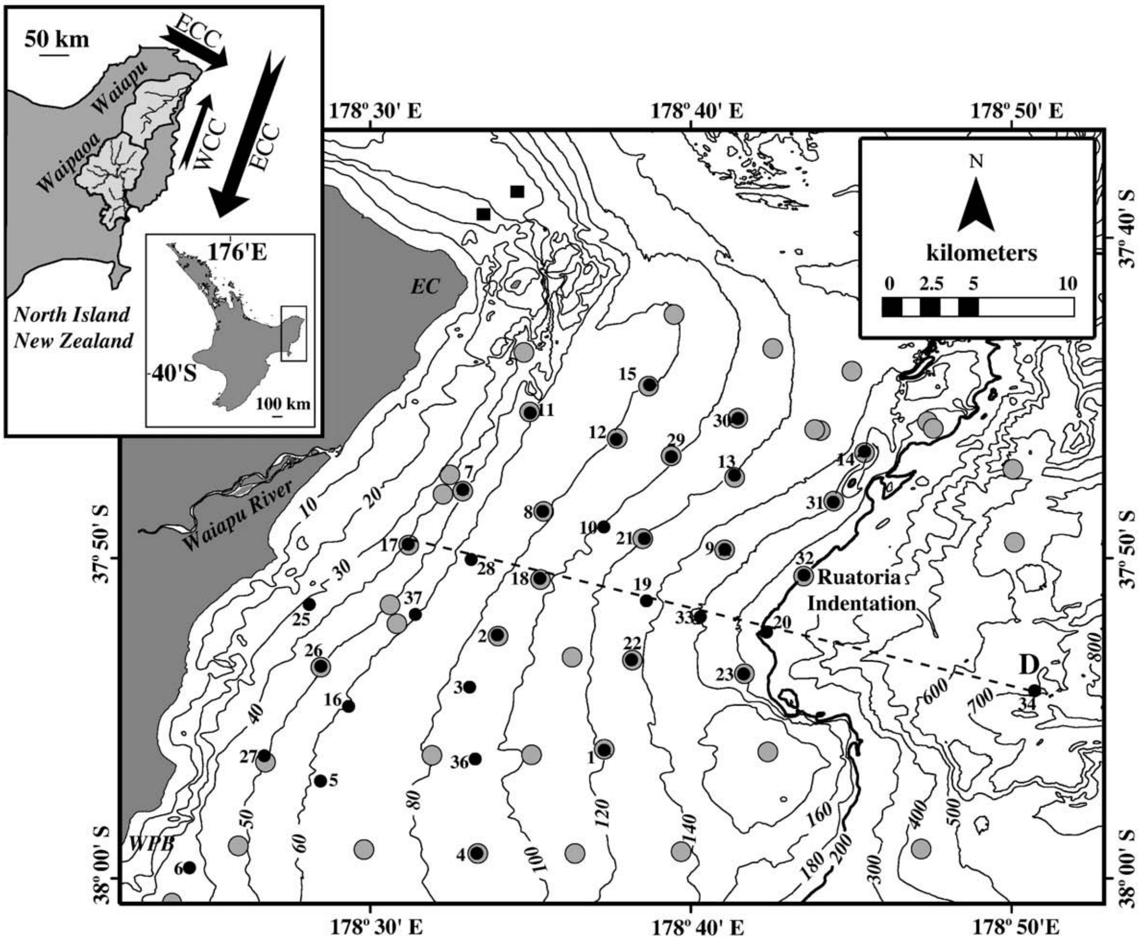

Fig. 1. Box and Kasten core distribution for the August, 2003 (black circles) and May, 2004 (gray circles) cruises. Samples were collected as far south as Waipiro Bay (WPB). Sandy sediments collected to the north of East Cape (EC) identified by black squares. The dashed line delineates transect D. The shelf break is defined by the 200 m isobath. The inset shows the study location on the North Island, New Zealand. Currents are labeled ECC (East Cape Current) and WCC, (Wairarapa Coastal Current).

mechanism with specific depositional signatures (Wheatcroft and Drake, 2003; Mullenbach et al., 2004; Leithold et al., 2005; Sommerfield and Wheatcroft, 2007). In fact, descriptions of hyperpycnal and gravity flow deposits vary from muddy layers (Wheatcroft and Borgeld, 2000) to cross-bedded silts (Mullenbach et al., 2004) and even turbidite-like sequences with silty basal units (Sommerfield and Wheatcroft, 2007). It is likely that the variability of these depositional sequences is attributable to multiple combinations of transport processes contributing to event layer formation (Wheatcroft and Borgeld, 2000; Wright and Friedrichs, 2006; Ma et al., 2008).

The Waiapu River shelf (Fig. 1) is an ideal location to investigate transport mechanisms and their depositional products because the river has one of the highest sediment yields in the world with concentrations predicted to exceed the threshold for hyperpycnal transport at least once per year (Mulder and Syvitski, 1995; Hicks et al., 2004). Additionally, observed energetic waves and currents during floods contribute to the formation of gravity-driven flows on the shelf (Ma et al., 2008). As part of a larger study of sediment transport and deposition on the Waiapu River shelf (Addington et al., 2007; Kniskern, 2007; Wadman and McNinch, 2008, Ma et al., 2008), this paper discusses modern shelf accumulation patterns on multiple time scales, biological and physical mixing patterns, preservation of terrestrial flood signals, and retention of fine-grained fluvial sediments on the continental shelf. Deciphering the effects of dispersal mechanisms on sediment burial history may enhance our understanding of the exchange and burial of important chemical constituents, and the interplay between biological and physical processes in forming fine, cm-scale strata.

2. Regional setting

The collision margin between the Pacific and Australian plates offshore of eastern New Zealand plays a significant role in sediment delivery and deposition on the shelf. The East Cape region is characterized by actively uplifting ranges and basins that comprise the backstop and forearc basin of the Hikurangi subduction zone (Walcott, 1987; Lewis and Pettinga, 1993). The East Cape rivers (Fig. 1), including the Waipaoa, Uawa, and Waiapu, drain this area, delivering an estimate 55 Mt (Hicks and Shankar, 2003) of easily eroded Triassic to Pleistocene materials (Field and Uruski, 1997) to the continental shelf.

The shelf adjacent to these rivers is only ~20 km wide, and bounded on the seaward side by the Hikurangi Trough (Lewis et al., 1998; Collot et al., 2001; Lewis et al., 2004). The Ruatoria Indentation (Fig. 1), a scar from seamounts subducted 2 to 0.2 Ma and subsequent debris flows between 40 and 170 ka, defines the shelf break (Lewis et al., 1998; Collot et al., 2001). Transpression from the obliquely converging tectonic plates contributed to the formation of a synclinal basin on the shelf adjacent to the Waiapu River (Lewis et al., 2004). Faulting within the basin and shelf subsidence rates approaching 4 m/ka created enough space to accommodate ~1 km-thick Quaternary deposits and ~100 m of Holocene fill (Lewis et al., 2004). Neogene and Quaternary faulting within the basin constrained the main loci of deposition near the shelf break (Lewis et al., 2004).

The Waiapu River (Fig. 1) has one of the highest sediment yields in the world, 17,800 t/km^2/yr, due to high rainfall rates (averaging 2.4 m/yr), the highly erodible quality of the basin rocks, and frequent seismic destabilization of the landscape (Hicks et al., 2000, 2004). The annual suspended sediment load is 35 ± 14 MT/yr, which is large for a drainage basin of only 1734 km^2 (Hicks et al., 2003). For comparison, the muddy sediment load of California Rivers, excluding the rivers that empty into San Francisco Bay, is 42 MT/yr with a cumulative catchment area of a little less than 100,000 km^2 (Farnsworth and Warrick, 2005). Like other small mountainous rivers, the Waiapu River basin area is too small to attenuate rain runoff (Milliman and Syvitski, 1992), resulting in high-load floods. The largest flood to affect the Waiapu River area in the last 100 yr was Cyclone Bola in 1988, which resulted in peak freshwater discharge of 4624 m^3/s, an estimated peak suspended sediment concentration of 60 g/L, and a total event yield of 73–93 MT, over twice the average annual sediment load in only a few days (Hicks et al., 2004).

Seasonal climate and large-scale shelf currents may influence delivery, transport, and deposition on the Waiapu River shelf. For example, the annual flood season typically runs from June–September although major events can happen any time, e.g., Cyclone Bola occurred in March. In contrast, the highest wave energy is generally between April and July. Tripod measurements collected from May 2004 through October 2004 on the Waiapu River shelf indicated waves are energetic during, or shortly after floods, with r.m.s. (root mean squared) wave heights of 2.5 to 3.5 m and significant waves heights of 3.5 to 5 m (Ma et al., 2008), capable of resuspending muddy sediments at ~80 m water depth (Ma, pers. comm.). Recent work has indicated that gravity-driven flows on the Waiapu River shelf may be supported by strong along-shelf currents as well as energetic waves (Kniskern et al., 2006; Kniskern, 2007; Ma et al., 2008). Near-bed cross-shelf currents ~0.5 m/s correlated with strong along-isobath currents, suggesting the presence of current-supported gravity flows. Additionally, in some areas of the shelf, the slope exceeded the threshold for auto-suspending gravity flows (Friedrichs and Wright, 2004; Ma et al., 2008).

Offshore, the East Cape Current (ECC) flows south along the shelf break and upper continental slope (Chiswell, 2000) (Fig. 1). Cooler and fresher waters, inshore of the ECC, flow northward, and are a possible extension of the Wairarapa Coastal Current (Chiswell, 2000). These currents and the Wairarapa and Hikurangi eddies produced by the ECC may ephemerally affect outer shelf water circulation (Chiswell, 2000, 2003, 2005). A clockwise-circulating eddy observed offshore of East Cape indicated that currents were directed landward to the south of the Waiapu River mouth and offshore to the north of the river mouth (Chiswell, 2003, 2005). Tripod data from May through September 2004 indicated that there is an along-shore, northward flowing, depth-averaged current of ~6 cm/s (Ma et al., 2008).

3. Methods

Samples were collected during two cruises, the first aboard NIWA's (National Institute of Water and Atmospheric Research Ltd.) RV Tangaroa in August of 2003, and the second aboard the University of Hawaii's Kilo Moana in May 2004. A total of 35 Kasten cores, 28 multi-cores, and 63 box cores comprise the data set. Kasten cores, measuring a maximum 3 m in length, and multi-cores measuring a maximum 1 m length, were collected during August 2003, near the end of the annual flood season. Box cores, up to 0.5 m long, and 2 Kasten cores were collected in May 2004, during the seasonal period of high wave energy (Fig. 1).

X-radiographs, radioisotope activity profiles, organic carbon and nitrogen contents, and grain-size comprised the data collected from the cores. Kasten cores were first sub-sampled using plexiglass trays (30 cm long by 3 cm thick) in order to preserve sediment structure. These slabs of sediment were exposed to X-rays using a Medison portable X-ray unit at 20 mA and 60 kV for an average 16 s and then negatives were developed using Kodak Industrex Redipack™ film aboard the RV Tangaroa. The resulting X-ray negatives reflect differences in bulk density such that dark and light features represent relatively low-density and high-density sediments, respectively. Subsequent to X-ray processing, all cores were sub-sampled in 2-cm thick sections, with highest resolution at the top of the core, for grain-size, organic carbon and nitrogen, and radiochemical analyses.

X-radiographs, radioisotopes, and grain size were used to characterize sediment structure as well as indicate mixing and accumulation patterns on the shelf (e.g. Nittrouer et al., 1984; Kuehl et al., 1996; Hirschberg et al., 1996; Dellapenna et al., 1998). Differences in bulk density identified in the X-radiographs were a function of grain-size, water content, and sediment bedding due to physical and biological processes. The X-radiographs were used to interpret the relative impact of biological and physical mixing on the sediment record and to improve our interpretations of radioisotope, bulk carbon, and $\delta^{13}C$ data. Radioisotope profiles were analysed to interpret sediment mixing processes and accumulation rates on multiple time scales. For example, ^{7}Be, with a half-life, $t_{1/2}$, of 53 days, was used to infer deposition on time scales of several months, whereas excess ^{210}Pb, with a half-life of 22.3 yr, was used to quantify sediment accumulation on time scales of decades to 100 yr. Bomb produced ^{137}Cs ($t_{1/2}$ = 30.1 y) first appeared in sediments in 1954, and was used to identify sediment mixing and corroborate excess ^{210}Pb accumulation rates (Nittrouer et al., 1984). Atmospheric deposition and in-situ decay of ^{226}Ra (for ^{210}Pb) are the main sources of these radioisotopes in coastal waters, whereas particle scavenging and settling deliver radioisotope activity to the seabed (e.g. Bruland et al., 1974; Dukat and Kuehl, 1995; Srisuksawad et al., 1997).

Assuming secular equilibrium, excess ^{210}Pb activities were determined by measuring ^{210}Po, its grand-daughter. Dried samples were spiked with a known amount of ^{209}Po and partially digested in 16 N HNO_3 and 6 N HCl, resulting in the release of ^{210}Po from the fine fraction. Following the methods of Flynn (1968), the Polonium isotopes were plated onto silver disks suspended in the leachate. An estimation of ^{226}Ra-supported activities was allowed when total ^{210}Pb

Table 1
Surface (0–2 cm) sand, silt, and clay fractions for the August 2003 and May 2004 cruises

Kasten core #	August 2003 sand/silt/clay	May 2004 sand/silt/clay	Water depth (m)
1	2.2 / 51.2 / 46.6	0.8 / 67.0 / 32.2	117
2	0.1 / 50.5 / 49.3	0.7 / 58.8 / 40.5	84
3	0.0 / 39.5 / 60.4	N/A	82
4	1.6 / 54.5 /43.9	0.1 / 70.0 / 29.9	85
5	0.0 / 44.1 / 55.9	N/A	57
6	26.0 / 50.0 / 24.0	N/A	31
7	15.4 / 64.9 / 19.7	4.6 / 70.8 / 24.5	41
8	0.0 / 56.3 / 43.7	1.5 / 49.4 / 49.1	72
9	0.1 / 59.1 / 40.9	N/A	143
10	1.1 / 53.5 / 45.4	N/A	97
11	6.2 / 67.0 / 26.9	0.1 / 62.0 / 37.9	55
12	1.7 / 61.8 / 36.4	0.2 / 68.5 / 31.4	78
13	3.0 / 57.5 / 39.5	4.9 / 61.5 / 33.7	116
14	42.9 / 38.3 / 18.8	27.7 / 48.9 / 23.4	149
15	14.7 / 58.2 / 27.1	N/A	74
16	0.6 / 57.2 / 42.2	N/A	56
17	59.7 / 32.6 / 7.7	25.7 / 56.8 / 17.5	35
18	0.6 / 52.9 / 46.6	0.3 / 53.4 / 46.3	86
19	0.1 / 53.7 / 46.1	0.2 / 64.1 / 35.7	132
20	4.4 / 47.0 / 48.6	8.0 / 49.4 / 42.6	201
21	0.7 / 53.3 / 46.0	2.1 / 55.3 / 42.6	118
22	0.5 / 51.8 / 47.8	0.9 / 48.2 / 50.9	131
23	34.0 / 39.4 / 26.7	21.6 / 54.5 / 23.9	165
25	8.2 / 67.5 / 24.3	N/A	26
26	0.7 / 72.5 / 26.8	0.3 / 70.9 / 28.8	44
27	3.8 / 65.3 / 31.0	5.8 / 54.2 / 40.0	44
29	5.5 / 58.7 / 35.9	7.0 / 55.3 / 37.7	94
30	9.8 / 58.9 / 31.3	22.6 / 43.4 / 34.0	103
31	7.4 / 59.1 / 33.5	7.3 / 68.7 / 24.0	157
32	36.6 / 39.7 / 23.6	28.4 / 49.9 / 21.7	200
33	0.6 / 51.6 / 47.8	4.3 / 64.1 / 31.6	156

Cores are identified by the August 2003 locations. Water depths are listed to emphasize that sandy surface sediments were primarily found at shallow water depths (<50 m), and at the shelf break (>140 m).

activities dropped to low, uniform levels at depth in the core. Where this supported activity could not be determined, an average value from the shelf was substituted. The supported level was subtracted from the total ^{210}Pb activity to get an excess ^{210}Pb value. Both ^{137}Cs and ^{7}Be activities were measured using a planar high purity germanium detector coupled with a multi-channel analyzer. Approximately 70–90 g of wet sediment was packed into a petri dish, and then gamma radiations were measured for 24–48 h.

The elemental and isotopic composition of organic matter was determined using an Isotope Ratio Mass Spectrometer (IRMS) at the University of California, Davis, Stable Isotope Facility. Samples from a single core, KC18, were dried, acidified with 10% HCl to remove inorganic carbon, and dried again before a sub-sample was transferred into methanol-rinsed tin capsules. Results included δ^{13}C, and total organic carbon and total nitrogen, which were used to determine the composition of bulk sedimentary organic matter (Leithold and Hope, 1999; Goni et al., 2006).

Waiapu River shelf surface (0–2 cm) sediments were analyzed in order to determine where muddy sediments were concentrated on the shelf. Sediments were wet sieved through a 63 µm sieve to separate the sand and mud fractions and then standard pipette methodology was used to determine the relative amounts of silt and clay. Higher-resolution analyses were performed on KC18 for comparison with ^{210}Pb and total carbon data using a Sedigraph 5100 at the Skidaway Institute for Oceanography Sedimentology Lab.

4. Results

4.1. Sedimentary texture and structure

Surface (0–2 cm) grain-size data revealed that Waiapu River shelf sediments are composed of mostly silt and clay sized particles with some sandy sediments found at shallow water depths (30–40 m) and along the shelf break (140–200 m) (Table 1). Muddy sediments were dominant between 50–140 m water depths. A subset of the May 2004 data re-occupied August 2003 locations (Fig. 1, Table 1). The small differences in average surface sample grain size between the two cruises generally were not significant and were attributed to spatial heterogeneity rather than temporal variability (Table 1).

Kasten core penetration depths, with greater core length used as an indicator of muddy or poorly consolidated muddy sediments, suggested that muddy sediment distribution was patchy at water depths shallower than 80 m and that the muddy mid-to outer-shelf deposit was oriented obliquely along-shelf (Fig. 2; Tables 1 and 2). Several times the Kasten corer was deployed between 20 and 80 m water depths, but was unable to penetrate the sediment, suggesting that the seabed in these areas was not muddy or was consolidated sufficiently to prevent penetration. Cores collected at water depths shallower than 50 m tended to be shorter than 40 cm (Fig. 2). Increasingly coarser (silty) sediments found at the base of the short cores indicated that the muddy surface sediments were underlain by materials too coarse or consolidated to permit Kasten core penetration. Kasten core penetration was greatest on the middle to outer shelf between 60 and 150 m water depth, gradually decreasing to the north and south. Muddy deposit thicknesses in the shelf break region varied over relatively small spatial scales. For example, core thicknesses between 140 and 200 m depth (Kasten cores 14, 31, 32, 9, 33, 23) ranged between 11 and 263 cm (Fig. 2; Table 2). This spatial variability at the shelf break was attributed to irregular bathymetry and the presence of small basins along the Ruatoria Indentation (Lewis et al., 1998; Collot et al., 2001; Addington et al., 2007).

Sedimentary structures in the X-radiographs implied that the dominant mixing mechanisms varied along and across the shelf (Fig. 3). At water depths shallower than 80 m, lamina and inter-

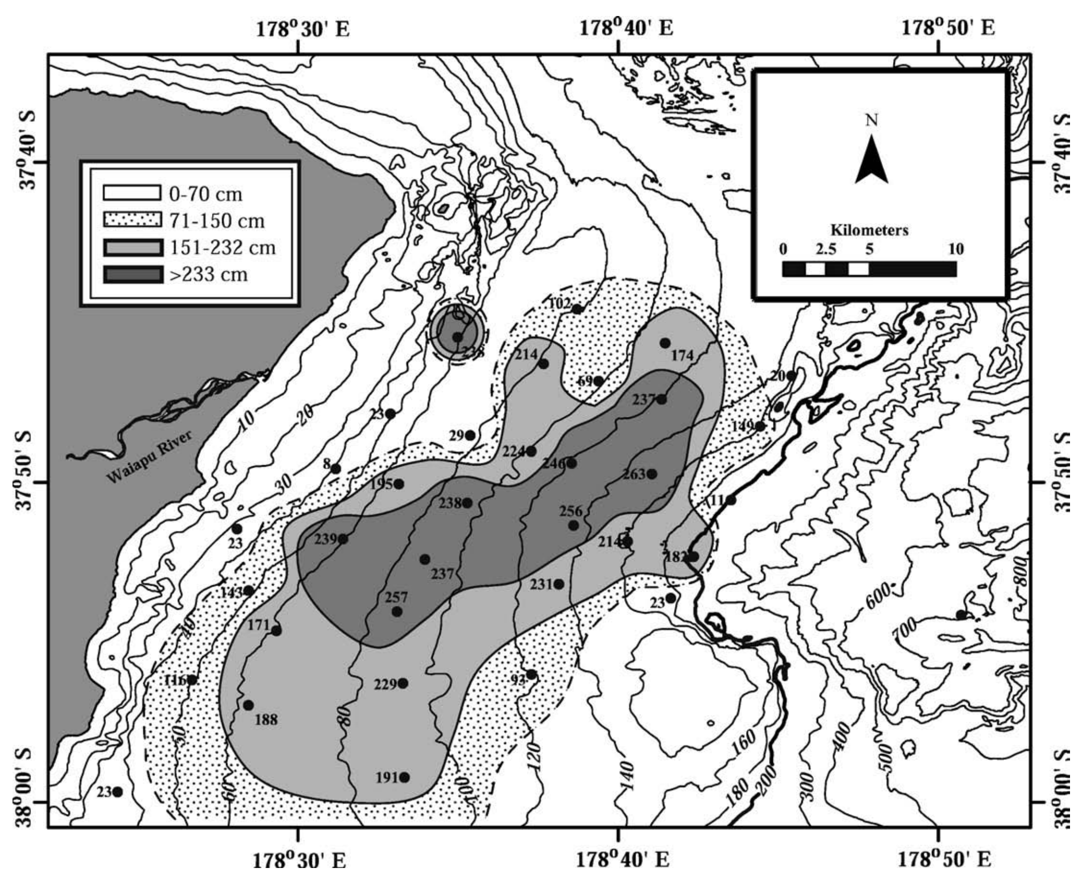

Fig. 2. Isopach map of Kasten core penetration, used as a proxy for muddy sediment content. A Natural Breaks (Jenks) algorithm was used to define the depth categories and draw the contours.

Table 2
Kasten core statistics

Kasten core	Accum. rate (cm/yr). No removal of low activities.	Accum. rate (cm/year). (Sommerfield and Nittrouer, 1999)	Event thickness (cm)	Accum. rate (cm/yr). Normalized to event thickness.	Core length (cm)	Maximum depth of $^{210}Pb_{xs}$
1	0.8	0.8	0	0.8	193	85
2	**4.3**	**3.0**	**62**	**1.4**	**237**	**135**
3	N/A	N/A	81.5	N/A	257	250
4	**0.9**	**0.9**	**14.5**	**0.8**	**191**	**80**
5	**2.1**	**1.1**	**15**	**1.0**	**188**	**130**
6	N/A	N/A	0	N/A	23	20
7	N/A	N/A	0	N/A	28	25
8	N/A	N/A	0	N/A	29	25
9	1.2	1.2	0	1.2	263	130
10	**2.0**	**1.8**	**32**	**1.4**	**224**	**165**
11	**N/A**	**3.5**	**2**	**3.4**	**238**	**100**
12	**2.0**	**1.7**	**43.5**	**0.9**	**214**	**105**
13	**1.8**	**1.6**	**15**	**1.4**	**237**	**110**
14	N/A	N/A	N/A	N/A	20	N/A
15	1.2	1.2	0	1.2	102	90
16	**2.6**	**2.5**	**37.5**	**1.7**	**171**	**165**
17	N/A	N/A	0	N/A	8	0
18	**2.1**	**2.4**	**47.5**	**1.9**	**238**	**150**
19	**3.9**	**1.4**	**10**	**1.0**	**256**	**150**
20	**1.2**	**1.1**	**19**	**0.9**	**182**	**105**
21	**2.5**	**2.1**	**17**	**1.9**	**246**	**170**
22	1.1	1.1	0	1.1	231	95
23	0.3	0.3	0	0.3	23	25
25	N/A	N/A	0	0	25	15
26	N/A	N/A	36	0	143	120
27	**0.9**	**1.0**	**5.5**	**0.9**	**116**	**95**
28	N/A	N/A	33	0	195	130
29	0.9	0.8	3.5	0.8	69	75
30	N/A	N/A	41	0	174	110
31	0.5	0.5	0	0.5	149	65
32	0.2	0.2	0	0.2	11	25
33	**1.1**	**1.0**	**18**	**0.8**	**214**	**125**
34	0.6	0.6	0	0.6	N/A	75
36	**1.4**	**1.7**	**21**	**1.3**	**229**	**109**
37	**4.7**	**2.0**	**27.5**	**1.4**	**239**	**114**

Non-steady state cores in bold. Accumulation rates were calculated using the CIC model, the modified CIC approach outlined by Sommerfield and Nittrouer (1999) and the background accumulation equation outlined in this paper. Event layer thickness, in the fourth column, is the total thickness of event layers in each core. The last two columns show the Kasten core lengths and maximum depths of excess ^{210}Pb.

bedded event beds ranging in thickness from a few mm up to 10 cm dominated physical sedimentary structures. Seaward of ~80 m water depth, the number of preserved laminations decreased radially from the Waiapu River mouth. Concomitantly, evidence of bioturbation increased radially with distance from the river mouth preserved between event beds. Sediments furthest from the Waiapu River mouth contained a few laminations interspersed with mottled and bioturbated sediments.

4.2. Radiochemical data

Generally, the longest cores also had the greatest thicknesses of excess ^{210}Pb. The elongate pattern of maximum excess ^{210}Pb depths showed that modern deposition was greatest on the mid- to outer-shelf just offshore of the Waiapu River mouth (Figs. 1, 2, and 4; Table 2). Modern depositional thicknesses were less on the inner shelf and shelf break region. It is important to note that both the pattern of maximum Kasten core penetration and maximum depth of excess ^{210}Pb were oriented not along-isobath, but oblique to bathymetry. The modern depocenter overlay and aligned with the subsiding synclinal shelf basin identified by Lewis et al. (2004) (Fig. 5).

Three depositional/mixing patterns were identified based on the shape of excess ^{210}Pb activity profiles: 1) cores shorter than 50 cm with uniform activity profiles; 2) cores between 50 and 200 cm long with logarithmic excess ^{210}Pb decay profiles; and 3) cores up to 250 cm long with non-steady-state profiles (Fig. 4). ^{210}Pb activity profiles are defined as non-steady state when activities do not decay logarithmically with depth, and are characterized by low activity sediments immediately above relatively higher activity sediments (e.g. Dukat and Kuehl, 1995; Sommerfield and Nittrouer, 1999).

The characteristics of the excess ^{210}Pb profiles changed along-shelf and across-shelf. Adjacent to the river mouth, the inner to mid-shelf cores, KC 7, 8, 17, 25, and 6, tended to be less than 50 cm, with uniform (i.e. mixed) excess ^{210}Pb profiles and activities ~1 dpm/g (Figs. 1 and 4; Table 2). Cores from the mid- to outer-shelf were longer and excess ^{210}Pb activities were found at greater depths, indicating a zone of muddy accumulation. Two types of excess ^{210}Pb activity profiles were identified on the mid- to outer-shelf: steady-state profiles that showed logarithmic decay with sediment depth, and non-steady-state profiles that showed variable excess ^{210}Pb activities with depth. Excess ^{210}Pb profiles for sites farthest from the Waiapu River mouth, KC 1, 9, 15, 22, 23, 31, 32, and 34, were steady-state. Of these, KC 32 and 23, collected along the shelf break, were less than 50 cm in length (Figs. 1 and 4; Table 2). A steady-state profile for a core collected from the slope, KC34 collected at 693 m water depth, indicated that some sediment is bypassing the shelf and accumulating on the slope (Figs. 1 and 4; Table 2).

The non-steady state profiles were characterized by a general decrease in excess ^{210}Pb activity with core depth, interspersed with sediment layers that displayed significantly lower activities than the activities above and below the sample (Fig. 4). A maximum 10% overlap of activity error bars was allowed for those samples identified near or within a low activity layer. These low activity layers, defined by low excess ^{210}Pb activities and constrained by X-radiographs, varied in thickness from a few centimeters up to 41 cm thick (Table 2). For those few instances where no visible boundary could be identified in the X-radiograph, then the boundary was defined as the mid-point between a low excess ^{210}Pb activity sample and the nearest high activity sample provided the intervening distance was no larger than 10 cm. Laminations dominated the X-radiographs of the non-steady state profiles, whereas X-radiographs from cores with steady-state profiles were more bioturbated with fewer physically-produced laminations (Figs. 3 and 4).

Accumulation rates for the steady state cores were calculated using a least squares regression assuming that there was no biological mixing below a surface mixing layer (Nittrouer et al., 1984; Appleby and Oldfield, 1992). The rates for the steady state cores ranged from 0.2 cm/yr to 1.2 cm/yr, averaging 0.7 ± 0.4 cm/yr (Fig. 4; Table 2). Three different methods were used to calculate accumulation rates on those ^{210}Pb profiles that were characterized as non-steady state. First, we calculated accumulation rates by running a least squares linear regression through all the excess ^{210}Pb data (Nittrouer et al., 1984; Appleby and Oldfield, 1992). Secondly, we calculated rates by removing the low ^{210}Pb activities from the data and using a least squares linear regression of the log for excess ^{210}Pb; a modified version of the Constant Initial Concentration (CIC) model used by Sommerfield and Nittrouer (1999) on non-steady ^{210}Pb profiles on the Eel River shelf (Nittrouer et al., 1984; Appleby and Oldfield, 1992). The third approach removes the low activity values as well as the thickness of the event bed identified using the excess ^{210}Pb profile and X-radiographs. On average, area weighted accumulation rates varied little: 1.3 ± 0.1 cm/yr, 1.1 ± 0.1 cm/yr, and 0.9 ± 0.1 cm/yr, respectively (Table 2). Differences in accumulation rates for each core, however, varied greatly and will be discussed in Section 5.2. Accumulation rates were not calculated for cores on the shelf when the majority of the sediment profile was dominated by low excess ^{210}Pb activity layers (e.g. KC 28, 30, 3, and 26) or the profile was short with uniformly low activities (e.g. KC 6, 7, 8, 17, 25, and14; Table 2).

We were unable to use ^{137}Cs to corroborate the accumulation rates calculated from the excess ^{210}Pb profiles or to assess biological/physical mixing rates because activities were often very low, or were

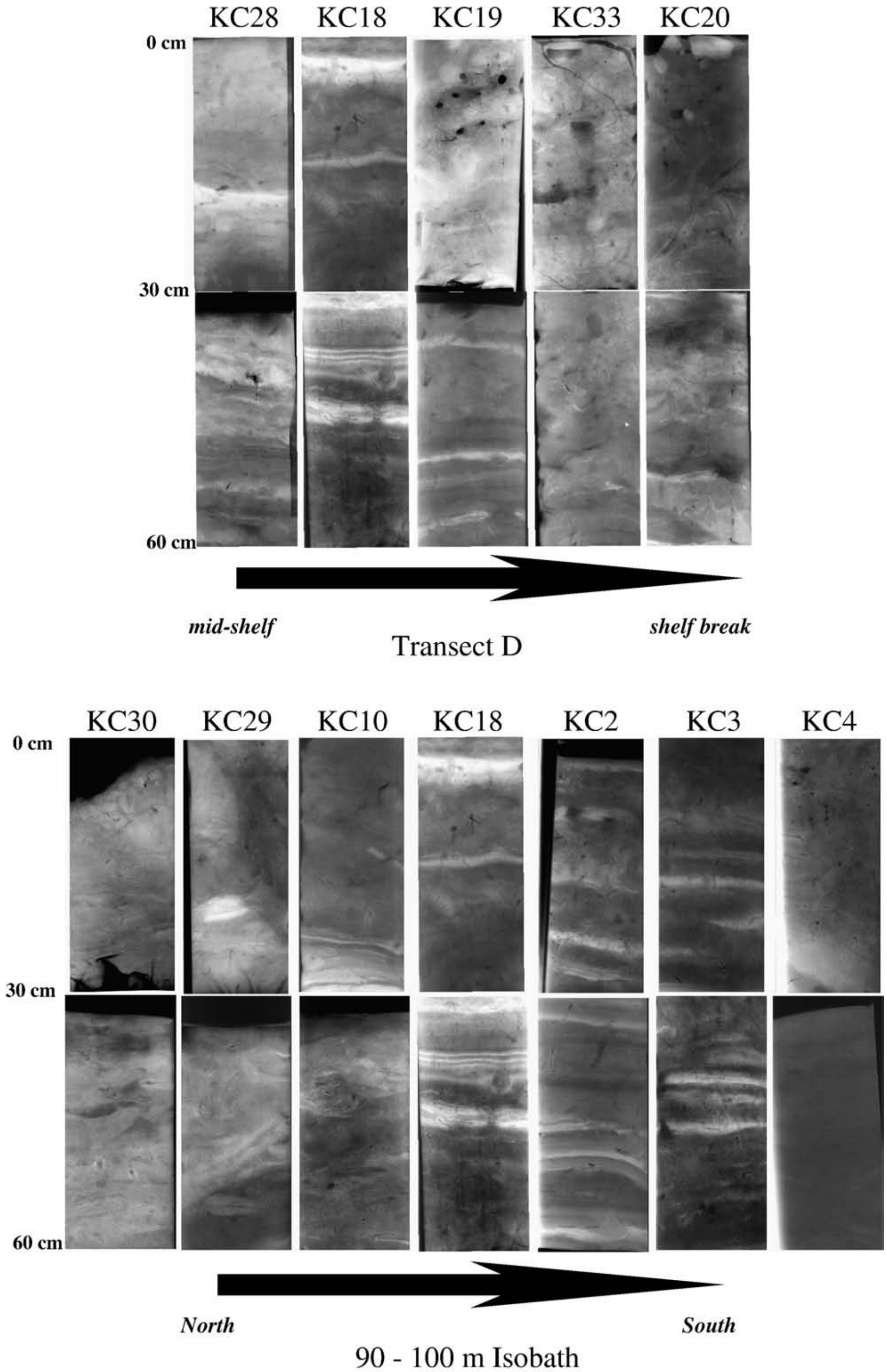

Fig. 3. X-radiograph negatives from Transect D and from along the 90–100 m isobath show increasing bioturbation across-shelf and to the north and south of the Waiapu River mouth (see Fig. 1).

below minimum detectable limits (~0.02 dpm/g). Surface sediments from the Waiapu River shelf revealed that the presence of ^{137}Cs was patchy, with low activities. One steady-state core (KC 9) was chosen for an in-depth analysis of ^{137}Cs to ascertain its potential to corroborate ^{210}Pb accumulation rates. The ^{137}Cs activities within the core were too low to identify either the first appearance of ^{137}Cs or the 1963 peak, presumably reflecting low Southern Hemisphere bomb fallout (Tsumune et al., 2003) and/or dilution of the signal by the extremely high Waiapu River yield (Kuehl et al., 2004). Further examination of the cores for ^{137}Cs was not attempted based on these results.

Measurements of ^{7}Be activities in surface samples (0–2 cm) from the August and May cruises indicated deposition of river-derived materials within 4 to 5 months of sampling (Fig. 6). Highest activities (~2 dpm/g) were found at shallower water depths, less than 90 m. Most cores collected from deeper waters had no detectable ^{7}Be activity. Measured activities ranged from 0.3–1.8 dpm/g with an average of 0.8 ± 0.5 dpm/g. The May, 2004 cruise revealed a larger area

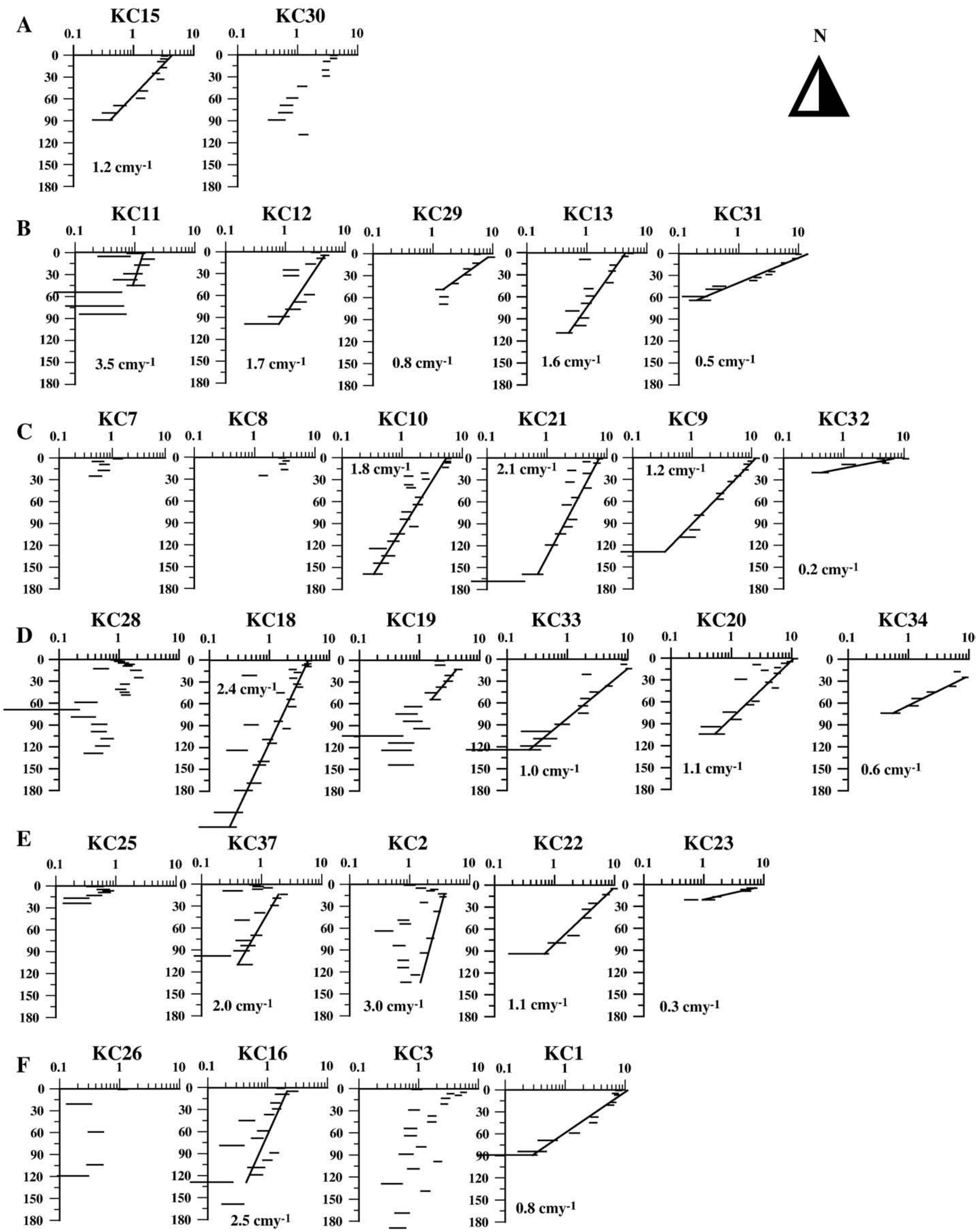

Fig. 4. Excess ^{210}Pb profiles for the Waiapu River shelf, transects A through F oriented with North at the top of the figure. (see Fig. 1). Apparent excess ^{210}Pb accumulation rates were calculated by removing the low excess ^{210}Pb values.

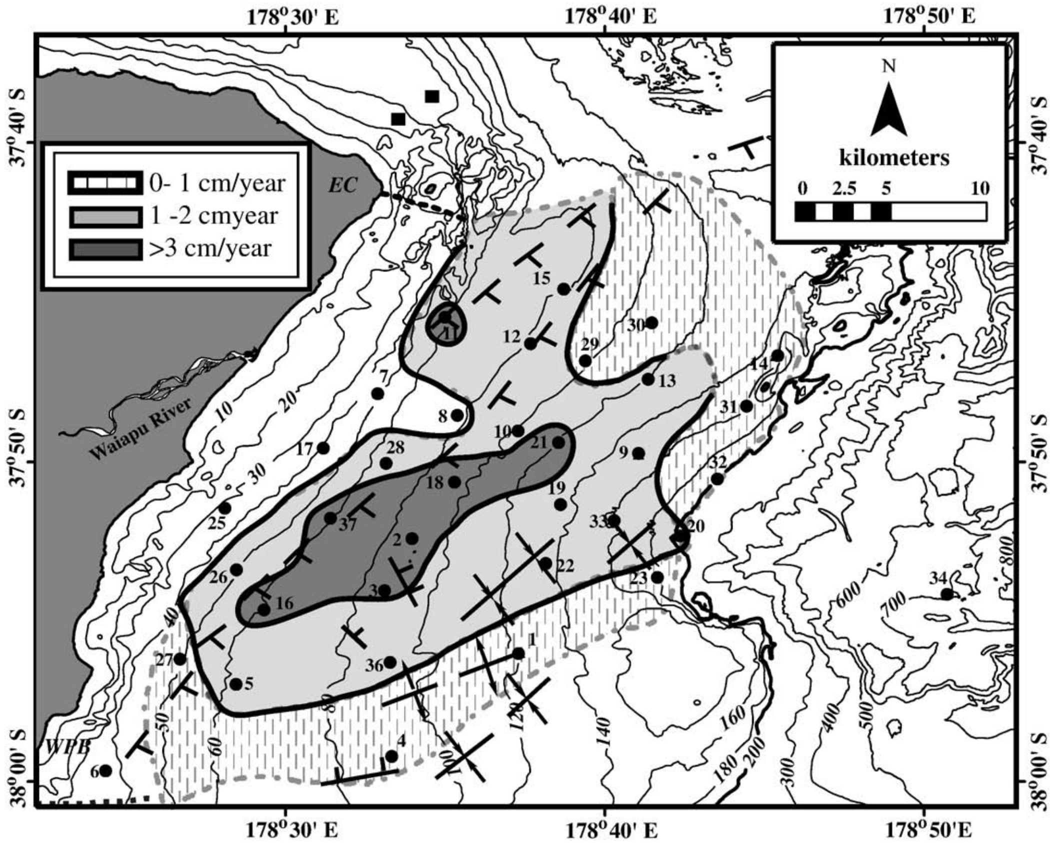

Fig. 5. Sediment accumulation patterns on the shelf. Dashed lines mark estimated boundaries of the shelf budget area. The budget area is constrained by East Cape (EC) to the north, Waipiro Bay (WPB) to the south, and the shelf break (here defined by the 200 m isobath) to the east. Fault and fold lines delineating the Waiapu River shelf basin are from Lewis et al. (2004). Locations represent Kasten cores from August 2003 and May 2004 (36 and 37).

of ^{7}Be deposition than the August cruise, due either to the larger sampling area in May, 2004, more recent sediment delivery, or varying patterns of sediment distribution.

4.3. Geochemical data

To better establish the provenance of the low ^{210}Pb activity layers, bulk carbon and nitrogen, and δ^{13}C were measured in core KC18 from the outer shelf (Fig. 7). Bulk organic carbon, atomic C/N, and δ^{13}C data indicated that the sediments on the shelf reflected mixed terrestrial and marine sources (Fig. 8). Organic carbon weight percent for KC18 varied between 0.35–0.73%, and generally fell within the 0.5–0.6% range observed by Leithold et al. (2006) for suspended sediment in the Waiapu River. The average δ^{13}C and C/N values for the core were −24.8 ±0.4‰ and 10.7±0.9‰, respectively, indicating that the sediments were a mixture of mostly terrestrial and marine carbon (Leithold and Hope, 1999; Leithold et al., 2006). Down-core variations in C/N ranged from 9.6–13.8, and δ^{13}C from −25.87 to −24.35, mirroring the pattern of variability observed in the excess ^{210}Pb activity profile (Fig. 7).

5. Discussion

5.1. Formation of low excess ^{210}Pb activity layers

We analyzed one core from the Waiapu River shelf to assess (1) the physical and chemical properties of the low excess ^{210}Pb activity layers and (2) whether we could identify the transport mechanism(s) that produced the flood event layers. The low excess ^{210}Pb activities found in KC18 were compared with grain-size, carbon content, and X-radiographs (Figs. 7, 9, and 10). The data suggested two pathways of emplacement: 1) rapid transport and deposition during floods resulting in low excess ^{210}Pb activities and terrestrial carbon values (Sommerfield and Nittrouer, 1999; Addington et al., 2007) and 2) slower transport and deposition such that bioturbation rates exceeded burial rates resulting in higher excess ^{210}Pb activities and mixed marine-terrestrial carbon values.

Grain-sizes for sediments from low activity layers were compared with grain-sizes from layers that did not exhibit low excess ^{210}Pb activities (Fig. 9 A and B). Although there appeared to be a weak relationship (r^2=0.54) between grain size and excess ^{210}Pb activity, it was not sufficient to produce the observed low activity layers. A decay-corrected profile was calculated by applying the accumulation rate to the profile, thereby making it easy to identify the anomalous low activity layers. The decay-corrected profile, normalized by the clay fraction, showed that down-core variability in grain size could not account for the low activity layers (Fig. 9 B). Had the grain-size affected ^{210}Pb adsorption, the normalized profile in Fig. 9 B would be straight relative to the uncorrected profile.

The low ^{210}Pb activity data did not always correspond with laminations or bedding in the X-radiographs, and not all laminations exhibited low ^{210}Pb activities (Fig. 10). Sediments at 21 cm and 84–89 cm were associated with darker, finer, laminations, whereas the other flood event layers were associated with lighter, coarser, laminations. There was a ~5 cm region of error in correlating X-radiographs with grain-size data, which were collected from the Kasten core rather than the X-radiograph sampling trays. This error was estimated by comparing a subset of X-radiographs with photographs of the Kasten cores prior to sampling. Additionally, the 2-cm core sampling interval was too coarse to accurately characterize changes in grain size within the event layers.

To assess whether we could match the event layers with a particular transport mechanism, we applied a grain-size criteria for event deposits used by Wheatcroft and Drake (2003) (Fig. 10). The results

Please cite this article as: Kniskern, T.A., et al., Sediment accumulation patterns and fine-scale strata formation on the Waiapu River shelf, New Zealand, Mar. Geol. (2009), doi:10.1016/j.margeo.2008.12.003

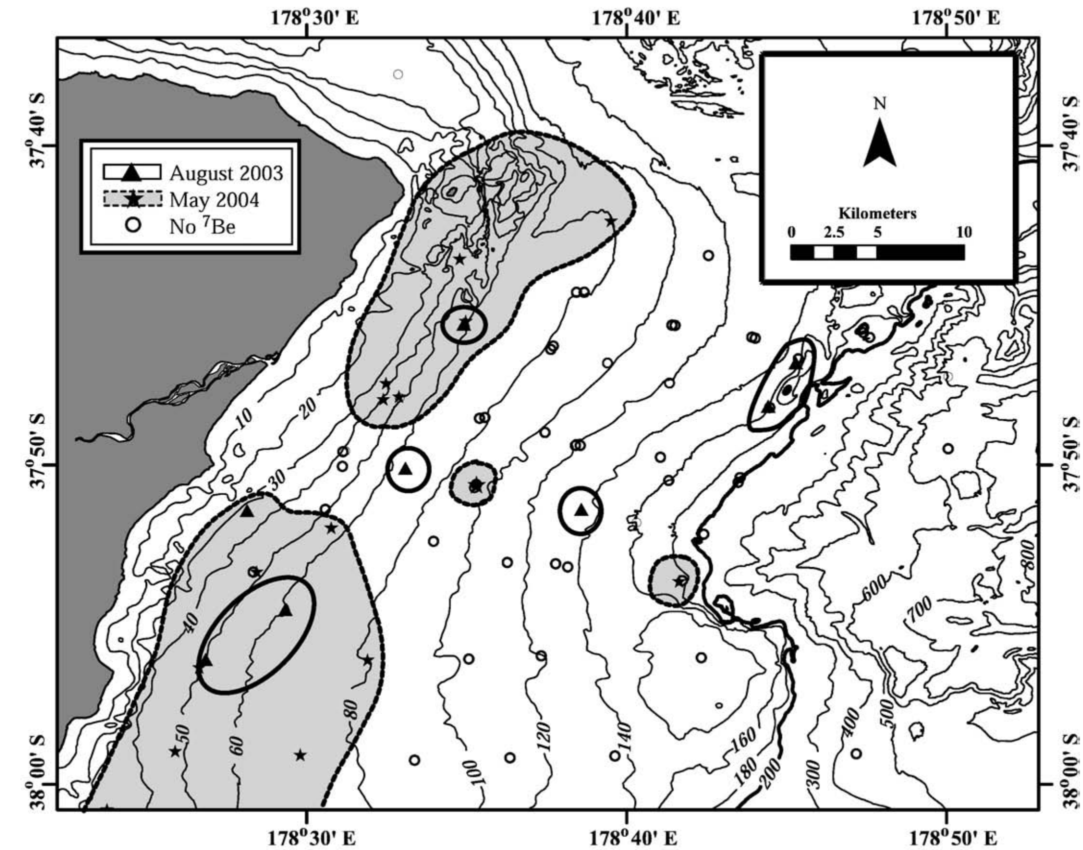

Fig. 6. The presence of ^{7}Be in surface sediment (0–2 cm) during the August 2003 and May 2004 cruises is represented by triangles and stars, respectively. The areas where ^{7}Be was found during the August 2003 cruise are outlined with a solid line, whereas areas identified in the May 2004 cruise are outlined with a dashed line and shaded gray.

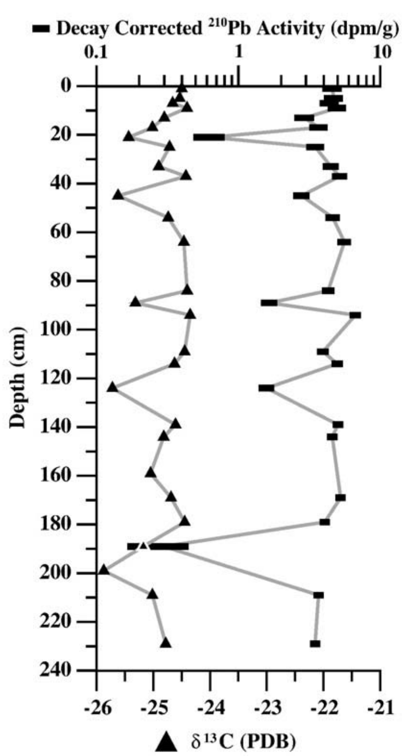

Fig. 7. Depth profiles of δ^{13}C and decay-corrected excess ^{210}Pb for KC18, the location of which is on Fig. 1. Excess ^{210}Pb has been decay corrected by applying the calculated accumulation rate to the activity profile.

suggested that multiple transport mechanisms were responsible for the low ^{210}Pb activity layers. Some of the low activity layers were finer and some were coarser than the mean weight percent of the <20 µm

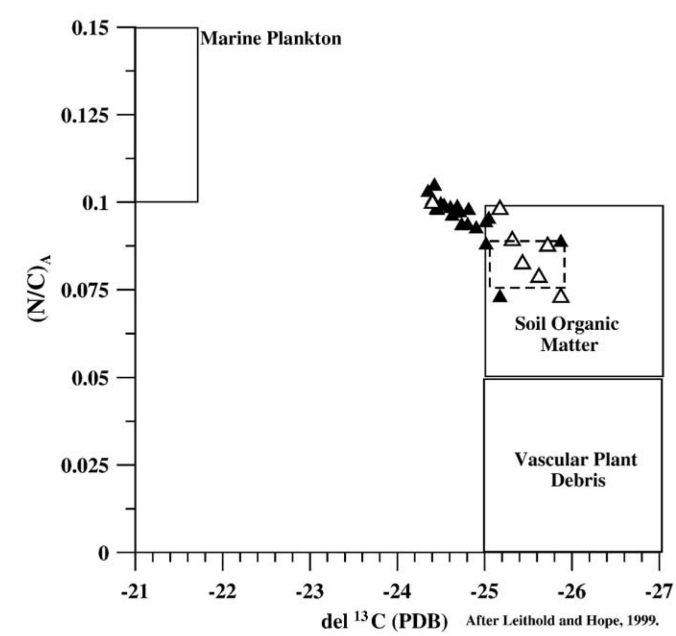

Fig. 8. Atomic ratio of N/C versus δ^{13}C. Open and closed triangles represent event layers and non-event layers from KC 18, respectively. The boxes outline ranges for marine plankton, soil organic matter, and vascular plant debris identified by Leithold and Hope (1999). The dashed lines represent the ranges of N/C and δ^{13}C measured in the Waiapu River by Leithold et al. (2006).

Please cite this article as: Kniskern, T.A., et al., Sediment accumulation patterns and fine-scale strata formation on the Waiapu River shelf, New Zealand, Mar. Geol. (2009), doi:10.1016/j.margeo.2008.12.003

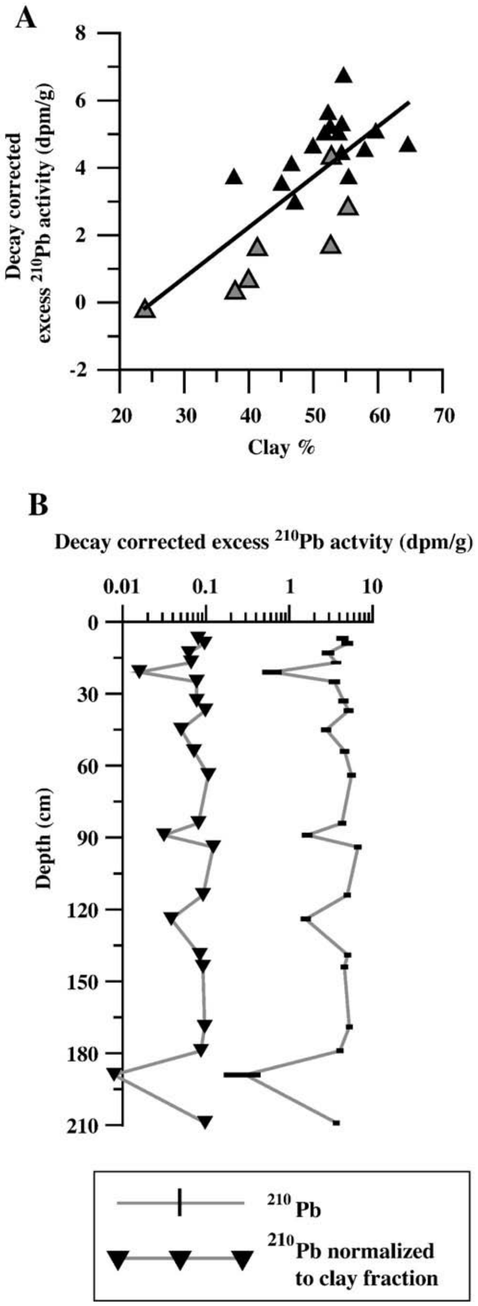

Fig. 9. A) Plot of excess ^{210}Pb versus the clay fraction for KC18. Gray triangles represent samples from event layers; black triangles are from non-event layers. B) Excess ^{210}Pb activities are decay corrected and normalized to clay fraction.

fraction (Fig. 10). The finer layers may represent wave- or current-initiated gravity-driven flow during floods. The coarser sediments may represent gravity-driven flows or simply represent wave or current resuspension into the water column following a flood or reflect different compositions as a result of supply or winnowing. For example, the contribution of material from landslides increases with storm intensity (Hicks et al., 2004), potentially affecting grain size distributions and organic carbon composition (Leithold et al., 2006).

The range in observed atomic C/N and δ^{13}C values for the identified flood events reflected various combinations of sediment delivery mechanisms and/or changes in basin sediment sources (Leithold and Blair, 2001; Leithold et al., 2006; Lloyd, 2007) (Figs. 7 and 8). Bulk atomic C/N ratios of suspended sediments in the Waiapu River ranged from 11.50 to 13.13, while δ^{13}C values ranged between −25.81 to −25.16‰ (Leithold et al., 2006). The δ^{13}C data from the event layers in KC18 fall within the range observed by Leithold et al. (2006) excluding the sample at 83–85 cm. Only samples taken at 20–22, 43–45, and 198–200 cm fall within the atomic C/N ranges, but the remaining event layers are still relatively riverine in value compared to those samples not associated with a low excess ^{210}Pb flood event layer (Figs. 7 and 8). The event layers displaying more mixed terrestrial/marine carbon values (more positive δ^{13}C) may reflect increased landsliding during those events or post-depositional reworking (Gomez et al., 2004; Lloyd, 2007). The event layers with relatively greater negative δ^{13}C, more terrestrial, values may represent storms during which gullies contributed more to the fluvial load (Gomez et al., 2004; Lloyd, 2007).

The carbon, grain size, and ^{210}Pb data suggest two pathways of emplacement: 1) rapid transport and deposition during floods resulting in low excess ^{210}Pb activities and terrestrial carbon values (Sommerfield and Nittrouer, 1999; Addington et al., 2007) and 2) slower transport and deposition such that bioturbation rates exceed burial rates resulting in higher excess ^{210}Pb activities and mixed marine-terrestrial carbon values. From other studies we know that waves and currents on the shelf were strong enough to support gravity-driven transport in the wave-current boundary layer both during and after floods (Kniskern, 2007; Ma et al., 2008). Although there was insufficient tripod data to evaluate whether auto-suspension is important on the Waiapu River shelf, some parts of the shelf do exceed the critical slope of 0.01 (Friedrichs and Wright, 2004).

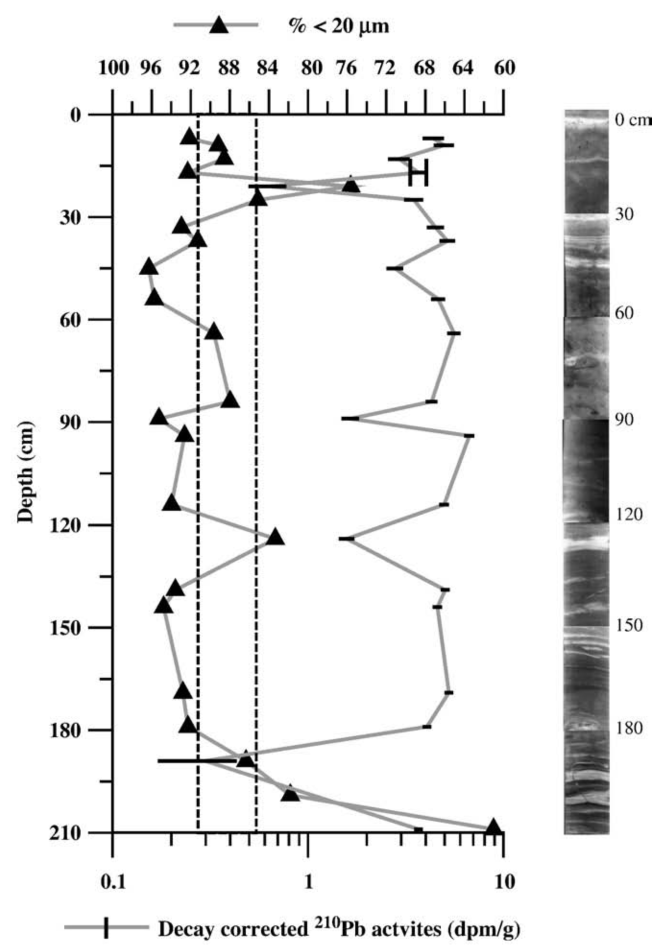

Fig. 10. The fraction finer than 20 µm is plotted relative to mean grain-size for KC18 (after Wheatcroft and Drake, 2003). The corresponding decay corrected excess ^{210}Pb activities and X-radiographs are plotted for easy identification of the event layers.

Please cite this article as: Kniskern, T.A., et al., Sediment accumulation patterns and fine-scale strata formation on the Waiapu River shelf, New Zealand, Mar. Geol. (2009), doi:10.1016/j.margeo.2008.12.003

5.2. Calculating ^{210}Pb accumulation rates

The sum thicknesses of event layers, as indicated by the grain size, δ^{13}C, C/N, and ^{210}Pb profile analyses, represented a significant fraction of the modern (last 80–100 yr) sediment record. The effects of these low excess ^{210}Pb layers on calculated accumulation rates were sufficient to require further investigation. The Waiapu River shelf accumulation rates calculated by removing the low excess ^{210}Pb values varied 1–63% (mean 20%) from accumulation rates calculated without removing the low activity layer values, a factor of two greater than the maximum 10% difference observed on the Eel River shelf (Table 2) (Nittrouer et al., 1984; Appleby and Oldfield, 1992; Sommerfield and Nittrouer, 1999). Fourteen out of the 16 identified non-steady state profiles varied by more than 10% between the two approaches, and were significantly different. The lower event layer ^{210}Pb values observed on the Waiapu River shelf could be caused by either shorter residence times in the water column prior to deposition, lower bioturbation rates post-deposition, a greater proportion of suspended sediments to available ^{210}Pb in the water column relative to the Eel River shelf, greater preservation of event layers on the shelf, or a combination.

To assess the relative contributions of event and hemipelagic delivery to the seabed, we calculated a background, or hemipelagic, accumulation rate. The thickness of the event layer as well as the low excess ^{210}Pb activities were removed from the profile before applying a least squares linear regression (Table 2). There was no significant difference in the average area weighted shelf accumulation rates produced by the background accumulation method, 0.9±0.1 cm/yr, and the method used by Sommerfield and Nittrouer (1999), 1.1± 0.1 cm/yr (Table 2). The difference in the two approaches does, however, provide an idea of how much the sediment record was influenced by event-related deposition for each location. Background accumulation rates for the 16 identified non-steady state cores were an average 21±14% lower than accumulation rates calculated by removing only the low excess ^{210}Pb activities (e.g. Sommerfield and Nittrouer, 1999). The accumulation rates for over half of the non-steady state cores were statistically different, suggesting that our interpretation of these event layers can significantly impact modeling of accumulation rates.

Further comparison of the two approaches revealed that event layer preservation increased with increasing background accumulation rate, suggesting that deposition from dilute suspension was important for preservation on the shelf as well as deposition by gravity flows. Fewer event layers were identified in regions of the shelf where background accumulation was less than 1 cm/yr (Figs. 3 and 4; Table 2). At water depths greater than 130 m, fewer observed event layers may indicate either that gravity-driven transport is not a dominant transport mechanism here and/or that lower accumulation rates result in increased transit time through the surface mixing layer and reworking by benthic organisms (Nittrouer and Sternberg, 1981; Wheatcroft, 1990; Wheatcroft and Drake, 2003, Bentley et al., 2006). An alternate explanation is that suspended sediments were possibly removed from the outer shelf by the ECC, which, with a volume transport of 10–20 Sv (Chiswell and Roemmich, 1998), could significantly influence suspended transport and deposition on the outer shelf and slope.

5.3. Sediment trapping efficiency

The boundaries of the shelf for the purposes of estimating shelf trapping efficiency were determined using data from this study and Lewis et al. (2004). The offshore extent of the shelf was defined by the 200-m isobath on the east. The northern and southern boundaries were determined using a combination of observations from this study (Table 2; Figs. 4 and 5) and the observed shelf basin sediment thicknesses from Lewis et al. (2004). The southern boundary, near Waipiro Bay (Fig. 5), was well defined by low accumulation rates and bioturbation structures. The northern boundary was less well defined because accumulation rates were still high at the northern-most extent of the study area. In addition, numerical modeling results indicated that sediments were primarily exported from the shelf to the north of the Waiapu River mouth (Kniskern, 2007), making it difficult to define the extent of the shelf deposit. The northern boundary was therefore based on the basin dimensions defined by Lewis et al. (2004) and the location of sandy sediments just to the north of East Cape (Fig. 1).

The trapping efficiency of fine-sediment was calculated using the apparent upper limit estimates calculated by removing the low excess ^{210}Pb values (Sommerfield and Nittrouer, 1999) (Fig. 4; Table 2). Apparent ^{210}Pb accumulation rates for each sub-region were averaged and applied over the whole. Porosity was held at 60% based on average values obtained from several cores at 50–100 cm depth, and are considered to be lower than what would be found at the surface of these cores. Annual fluvial delivery was assumed to be 35±14 MT/yr (Hicks et al., 2004). Based on this approach, we estimated that about ~23% of the sediments disgorged by the Waiapu River accumulated on the shelf between ~40–200 m water depths over the last 100 yr (Fig. 4).

Errors associated with this estimate of shelf retention included spatial interpolation of ^{210}Pb accumulation rates, errors associated with the calculation of the ^{210}Pb accumulation rates, assumption of a uniform porosity, identification of the shelf boundaries, the 40% uncertainty of the modern Waiapu River annual load (Hicks et al., 2003), and core compaction. The uncertainty of the fluvial load and porosity contributed to the largest errors. The fluvial load error resulted in a maximum trapping efficiency error of −6% to +16. Varying the uniform porosity from 60–90% resulted in an error of up to 17%. Assuming a maximum 28% of core shortening due to compaction (Mitra et al., 1999; Blomqvist, 1985) resulted in a 7% budget error.

Accumulation rate errors contributed minimally to variance in the estimate of shelf trapping efficiency, accounting for only 2% of the budget. We assessed accumulation rate errors using 1) the error of each ^{210}Pb datum and 2) the standard error of the slope of regression. Maximum and minimum accumulation rates produced using these two methods revealed an average error of +12%. When the accumulation rates were applied to the shelf budget, spatial interpolation significantly reduced the impact of the accumulation rate errors. Additionally, accumulation rates were compared to rates calculated by dividing the maximum ^{210}Pb penetration depth (Table 2) by 4–5 times the ^{210}Pb half-life, thereby increasing spatial resolution. The resultant trapping efficiency ranged from 19 –24%, adding little error to the original estimate of 23%.

Errors due to Kasten core sampling resolution and identifying the basin boundaries were difficult to quantify. Kasten core sampling resolution was most dense offshore of the Waiapu River mouth, transects C, D, and E, where the highest accumulation rates were identified. On average, the distance between sampling sites was ~3.5 km. Additional sampling would refine the 23% trapping efficiency estimate.

The depositional pattern and ^{210}Pb profiles indicated that most muddy sediments were only ephemerally deposited between 40 and 50 m water depths. Muddy sediments likely bypassed this region of the shelf because energetic waves and currents (Wright et al., 2006; Ma et al., 2008) moved the sediments offshore (Kniskern, 2007; Ma et al., 2008). Seismic data and vibracores collected from this region (up to 50 m water depth) revealed inter-bedded sands and muds to the south of the river mouth and massively emplaced sands and muds to the north of the river mouth (Wadman and McNinch, 2008).

Sediments not trapped on the shelf were likely transported to the north of the Waiapu River and across the shelf to the Ruatoria Indentation. Event layers identified in transect D cores from the shelf break (Figs. 1, 3, and 4) indicated that this area of the shelf was acting as a conduit for sediments to deeper waters. Sediments found in basins along the shelf break (Addington et al., 2007), and KC34 from this study suggest that Waiapu River sediments were transported beyond the shelf break. Numerical modeling results and tripod

Please cite this article as: Kniskern, T.A., et al., Sediment accumulation patterns and fine-scale strata formation on the Waiapu River shelf, New Zealand, Mar. Geol. (2009), doi:10.1016/j.margeo.2008.12.003

observations indicated that most sediments exported from the system were likely transported to the north of the river mouth, in the direction of the average along-shelf current (Kniskern et al., 2006; Kniskern, 2007; Ma et al., 2008).

The shelf deposit on the Waiapu River shelf is similar to the deposit on the Eel River shelf in several ways. Both retained an estimated ~20% of the muddy load on a relatively narrow shelf, only 15–20 km wide (Sommerfield and Nittrouer, 1999). Muds and sands are also trapped on the inner shelves of both systems (Crockett and Nittrouer, 2004; Wadman and McNinch, 2008). An estimated 6–13% of Eel River muds are trapped on the inner shelf (Crockett and Nittrouer, 2004), whereas 16–34% of muds are trapped on the Waiapu River shelf between 0 to 50 m water depth (Wadman, 2008). One distinct dissimilarity, however, is that the Eel River shelf deposit is aligned along-bathymetry, whereas the depocenter on the Waiapu River shelf cuts across bathymetry (Fig. 5). The Waiapu River shelf deposit location appears to be influenced by an underlying synclinal basin (Lewis et al., 2004). In this regard the Waiapu River shelf is similar to the Waipaoa River shelf (Fig. 1) where deposition is also significantly influenced by regional tectonics (Miller and Kuehl, in review).

5.4. Event layer preservation

To preserve an event layer, it must transit through a surface mixing layer on the seabed (Guinasso and Schink, 1975) quickly enough that the physical characteristics (grain size) of the event bed are not destroyed by subsequent bioturbation and/or physical reworking (Nittrouer and Sternberg, 1981; Wheatcroft, 1990; Wheatcroft and Drake, 2003). Once the event bed is advected through the surface mixing layer, it is considered preserved in the sediment record (Nittrouer and Sternberg, 1981; Nittrouer et al., 1984).

Generally, average continental shelf sediment accumulation rates (0.1 to1.0 cm/yr) are too low to completely limit mixing by benthic organisms (Boudreau, 1994; Wheatcroft and Drake, 2003). The surface mixing layer is typically commensurate with a zone of active bioturbation, between 5 and 30 cm thick, with bioturbation rates ranging from ~10–100 cm^2/yr (Wheatcroft and Drake, 2003, and references therein). Wheatcroft and Drake (2003) used the equation $T_m = [L_b - L_s/2]/S$ to measure how quickly half of the event layer is transited through the surface mixing layer, where the transit time of half of the event layer is T_m, L_b is the mixing layer thickness, L_s is the event bed thickness, and S is the accumulation rate. A comparison of the estimated transit times and observed event layer dissipation times on the Eel River shelf indicated that most flood/event layers (<8 cm) are not preserved there (Wheatcroft and Drake, 2003; Bentley et al., 2006).

The preservation of event layers and the distribution of bioturbation signals in the sediment record varied along and across the Waiapu River shelf as indicated by X-radiographs (Fig. 3). Event bed and lamina dominated sediment structure in areas with the highest background accumulation rates, whereas bioturbation structures were more prevalent in areas where background accumulation was less than 1 cm/yr (Figs. 3 and 4). High accumulation rates (area weighted average of 1.1±0.1 cm/yr) compared to those observed on the Eel River shelf (0.4 cm/yr; Wheatcroft and Drake, 2003), in conjunction with frequent flooding, have contributed to the preservation of thick (~20 cm) event beds on the Waiapu Shelf (Figs. 3 and 4).

Although we were not able to assess macrobenthic abundances on the Waiapu River shelf, studies on shelves with high accumulation rates, and/or frequent floods have revealed a relative paucity of benthos and subsequently low estimated biodiffusivity rates on shelves offshore of the Eel, Amazon, and Chianjiang Rivers (Rhoads et al., 1985; Aller and Stupakoff, 1996; Bentley and Nittrouer, 2003; Wheatcroft, 2006). To conservatively gauge event bed preservation potential, we applied mixing layer thickness and dissipation measurements (Db=10–100 cm^2/yr, average 29 cm^2/yr) from the Eel River shelf (Wheatcroft and Drake, 2003; their Fig. 5), and used an area-normalized Waiapu River shelf accumulation rate of 1.1 cm/yr. Applying Wheatcroft and Drake's (2003) Fig. 5 and a 1-D preservation potential model from Bentley et al. (2006) to the Waiapu River shelf suggested that some fraction of an event bed only a few centimeters (~4–6 cm) thick would be preserved with a 10–15 cm-thick surface mixing layer. For event beds thicker than the mixing layer thickness (when $L_s > L_b$) some fraction of the event bed is immediately preserved in the sediment record. The Wheatcroft and Drake (2003) equation can be modified such that $T_m = [L_b - (L_s - L_b)/2]/S$, thereby giving the transit time of half the thickness of the event bed not immediately advected through the surface mixing layer.

5.5. Long- vs. short-term accumulation

Radioisotope activities on the Waiapu River shelf indicated that sediment depositional patterns varied over long- and short-term time-scales. The presence of excess ^{210}Pb showed that sediments were deposited in waters deeper than 40 m water over the last 80 to 100 yr (Fig. 5). Accumulation rates and maximum penetration of ^{210}Pb showed a mid- to outer-shelf depocenter, between 80 m and 120 m water depth, just landward of the Holocene depocenter identified by Lewis et al. (2004). Sediments deposited only a few months prior to collection, however, revealed a very different spatial pattern (Fig. 6). Most samples containing detectable ^{7}Be were found between 30–80 m water depth, just landward of the longer-term ^{210}Pb depocenter (Figs. 5 and 6).

These depositional patterns indicated an apparent disconnect between short- and long-term transport and reworking processes. Recent deposition was generally confined to water depths shallower than 80 m for both cruises, suggesting that sediments were first deposited on the inner and mid-shelf and subsequently transported to deeper waters, where ^{210}Pb accumulation rates were highest. By the time sediments were redistributed to deeper waters, ^{7}Be activities may have been near the limit of detection. Other coastal systems have been observed to temporarily store sediments in shallower waters over time-scales of a week, followed by resuspension and transport to deeper waters (Sommerfield et al., 1999; Gerald and Kuehl, 2006). None have observed a depositional disconnect between ^{7}Be and ^{210}Pb depositional patterns (Sommerfield and Nittrouer, 1999; Sommerfield et al., 1999). This apparent discrepancy in depositional patterns could be due to either sampling schedule relative to depositional event and subsequent redistribution and/or differences in dispersal and redistribution due to variable weather and oceanic conditions.

Recent research on the Waiapu River shelf suggested that the relative strength of along shore currents and wave energy influenced sediment transport, initial deposition, and subsequent redistribution (Kniskern, 2007; Ma et al., 2008). Freshly dispersed sediments were temporarily trapped on the inner and mid-shelf when along-shelf currents were strong enough to confine the fresh water and sediment plumes to the inner shelf (Kniskern, 2007; Kniskern et al., 2008). Satellite imagery confirmed this configuration, showing buoyant plumes confined to shallow waters (e.g., Hicks et al., 2004). Sediments were deposited and resuspended on the inner shelf until wave energy was sufficiently stronger than along-shelf currents, resulting in rapid offshore sediment transport in gravity-driven flows (Kniskern et al., 2008). If along-shelf currents were weak and waves were energetic during a flood event, terrigenous sediments would quickly move to deeper waters, in effect bypassing the inner shelf (Kniskern, 2007). Under the latter conditions, ^{7}Be activities would likely be detectable at water depths >80 m.

6. Conclusions

1) Accumulation rates on the Waiapu River shelf were high, with an area weighted average of 1.1±0.1 cm/yr; ranging from 0.2–3.5 cm/yr.

Please cite this article as: Kniskern, T.A., et al., Sediment accumulation patterns and fine-scale strata formation on the Waiapu River shelf, New Zealand, Mar. Geol. (2009), doi:10.1016/j.margeo.2008.12.003

An estimated ~23% of muddy sediments delivered to the shelf during the last 100 yr were trapped on the adjacent shelf between 40 and 200 m depth. The remainder of the sediment was either trapped on the inner shelf, or transported to the north or beyond the shelf break.

2) Long-term accumulation patterns significantly differed from short-term patterns during the observed periods. Muddy sediments tend to be ephemerally deposited between 30 and 50 m water depths. Longer-term accumulation rates peaked between 80 and 120 m water depths.
3) Physical processes dominated sedimentary structures on the shelf. Beds of up to 20 cm thick were most often found on the mid-shelf. Bioturbation increased radially from the Waiapu River mouth as apparent accumulation rates decreased.
4) The non-steady-state nature of the ^{210}Pb signal on the mid- to outer shelf versus the steady state cores found at the shelf break and slope suggest multiple sediment delivery mechanisms influenced strata formation including dilute suspensions, gravity-driven flows, and water column resuspension. Event layers exhibited a distinctly terrestrial signal compared to non-event sediments. The number of event layers decreased from the mid- to outer-shelf. Steady-state profiles are likely a product of bioturbation and decreased event sediment delivery.
5) Grain-size criteria indicated that event layers, identified by low excess ^{210}Pb and carbon data, were potentially the product of multiple combinations of sediment transport pathways: river-initiated hyperpycnal plume, wave-or current supported gravity flows, and wave or current resuspension.

Acknowledgements

The authors thank the National Institute of Water and Atmospheric Research (NIWA) together with the scientific and ships crew of RV Tangaroa, and the University of Hawaii's RV Kilo Moana. Special thanks are extended to the people of the Ngati Porou Iwi, who graciously shared their land and culture. Comments by Murray Hicks, Chris Sommerfield, and Rob Wheatcroft greatly improved this paper. Our research was funded by the National Science Foundation, project number OCE-0326831 and Foundation for Research Science and Technology contract CO1X0203.

References

Addington, L.D., Kuehl, S.A., McNinch, J.E., 2007. Distinguishing sediment transport modes to the outer-shelf off the Waiapu River, New Zealand. Mar. Geol. 243, 18–30.

Aller, J.Y., Stupakoff, I., 1996. The distribution and seasonal characteristics of benthic communities on the Amazon shelf as indicators of physical processes. Cont. Shelf Res. 16, 717–751.

Appleby, P.G., Oldfield, F., 1992. Application of lead-210 to sedimentation studies. In: Ivanovich, M., Harmon, R.S. (Eds.), Uranium Series Disequilibrium, Applications to Earth, Marine and Environmental Sciences. Clarendon Press, Oxford, pp. 731–778.

Bentley, S.J., Nittrouer, C.A., 2003. Emplacement, modification, and preservation of event strata on a flood-dominated continental shelf: eel shelf, Northern California. Cont. Shelf Res. 23, 1465–1493.

Bentley, S.J., Sheremet, A., Jaeger, J.M., 2006. Event sedimentation, bioturbation, and preserved sedimentary fabric: field and model comparisons in three contrasting marine settings. Cont. Shelf Res. 26, 2108–2124.

Blomqvist, S., 1985. Reliability of core sampling of soft bottom sediment – an *in situ* study. Sedimentology 32, 605–612.

Boudreau, B.P., 1994. Is burial velocity a master parameter for bioturbation? Geochim. Cosmochim. Acta 58, 1243–1249.

Bruland, K.W., Koide, M., Goldberg, E.D., 1974. The comparative marine geochemistries of Lead ^{210} and Radium 226. J. Geophys. Res. 79, 3083–3086.

Chiswell, S.M., 2000. The Wairarapa coastal current. N.Z. J. Mar. Freshw. Res. 34, 303–315.

Chiswell, S.M., 2003. Circulation within the Waiararapa Eddy, New Zealand. N.Z. J. Mar. Freshw. Res. 37, 691–704.

Chiswell, S.M., 2005. Mean and variability in the Wairarapa and Hikurangi Eddies, New Zealand. N.Z. J. Mar. Freshw. Res. 39, 121–134.

Chiswell, S.M., Roemmich, D., 1998. The East Cape Current and two eddies: a mechanism for larval retention? N.Z. J. Mar. Freshw. Res. 32, 385–397.

Collot, J.-Y., Lewis, K., Lemarche, G., Lallemand, S., 2001. The giant Ruatoria debris avalanche on the northern Hikurangi margin, New Zealand: result of oblique seamount subduction. J. Geophys. Res. 106 (B9), 19271–19297.

Crockett, J., Nittrouer, C.A., 2004. The sandy inner shelf as a repository for muddy sediment: an example from Northern California. Cont. Shelf Res. 24, 55–73.

Dellapenna, T.M., Kuehl, S.A., Schaffner, L.C., 1998. Sea-bed mixing and particle residence times in biologically and physically dominated estuarine systems: a comparison of lower Chesapeake Bay and the York River Subestuary. Estuar. Coast. Shelf Sci. 46, 777–795.

Dukat, D.A., Kuehl, S.A., 1995. Non-steady-state ^{210}Pb flux and the use of ^{228}Ra/^{226}Ra as a geochronometer on the Amazon continental shelf. Mar. Geol. 125, 329–350.

Farnsworth, K.L., Milliman, J.D., 2003. Effects of climatic and anthropogenic change on small mountainous rivers: the Salinas River example. Glob. Planet. Change 39, 53–64.

Farnsworth, K.L. and Warrick, J.A., 2005. Sources of Fine Sediment to the California Coast: Computation of a 'Mud Budget', Interim Report to the California Sediment Management Working Group, California Dept. of Boating and Waterways, 128 pages.

Field, B.D., Uruski, C.I., 1997. Cretaceous–Cenozoic Geology and Petroleum Systems of the East Coast Region, New Zealand. Monograph, vol. 19. Institute of Geological and Nuclear Sciences, Lower Hutt, NZ.

Flynn, W.W., 1968. The determination of low levels of polonium-210 in environmental materials. Anal. Chim. Acta 43, 221–227.

Friedrichs, C.T., Wright, L.D., 2004. Gravity-driven sediment transport on the continental shelf: implications for equilibrium profiles near river mouths. Coast. Eng. 51, 795–811.

Gerald, L.E., Kuehl, S.A., 2006. Recent Sediment Dispersal and Preservation of Storm Events on the Continental Shelf off the Waipaoa River, NZ. Ocean Sciences Meeting, Honolulu, Hawaii. Abstract OS16A-29.

Gomez, B., Brackley, H.L., Hicks, M.D., Neff, H., Rogers, K.M., 2004. Organic carbon in floodplain alluvium: signature of historic variations in erosion processes associated with deforestation, Waipaoa River basin, New Zealand. J. Geophys. Res. 109, F04011 9 pages.

Goni, M.A., Monacci, N., Gisewhite, R., Ogston, A., Crockett, J., Nittrouer, C., 2006. Distribution and sources of particulate organic matter in the water column and sediments of the Fly River Delta, Gulf of Papua (Papua New Guinea). Estuar. Coast. Shelf Sci. 69, 225–245.

Griffiths, G.A., Glasby, G.P., 1985. Input of river-derived sediment to the New Zealand continental shelf. I. Mass. Estuar. Coast. Shelf Sci. 21, 773–787.

Guinasso, N.L., Schink, D.R., 1975. Quantitative estimates of biological mixing rates in abyssal sediments. J. Geophys. Res. 80, 3032–3043.

Harris, C.K., Traykovski, P.A., Geyer, W.R., 2005. Flood dispersal and deposition by near-bed gravitational sediment flows and oceanographic transport: a numerical modeling study of the Eel River shelf, nothern California. J. Geophys. Res. 110, C09025.

Hicks, M., Shankar, U., 2003. Sediment from New Zealand Rivers. NIWA Misc. Chart 236. NIWA, Wellington.

Hicks, D.M., Gomez, B., Trustrum, N.A., 2000. Erosion thresholds and suspended sediment yields, Waipaoa River Basin, New Zealand. Water Resour. Res. 36, 1129–1142.

Hicks, M., Shankar, U., McKerchar, A., 2003. Sediment yield estimates: a GIS tool. Water Atmos. 11, 26–27.

Hicks, D.M., Gomez, B., Trustrum, N.A., 2004. Event suspended sediment characteristics and the generation of hyperpycnal plumes at river mouths: east coast continental margin, North Island, New Zealand. J. Geol. 112, 471–485.

Hirschberg, D.J., Chin, P., Feng, H., Cochran, J.K., 1996. Dynamics of sediment and contaminant transport in the Hudson River Estuary: evidence from sediment distributions of naturally occurring radionuclides. Estuaries 19, 931–949.

Kineke, G.C., Woolfe, K.J., Kuehl, S.A., Milliman, J.D., Dellapenna, T.M., Purdon, R.G., 2000. Sediment export from the Sepik River, Papua New Guinea; evidence for a divergent sediment plume. Cont. Shelf Res. 20, 2239–2266.

Kniskern, T.A., 2007. Shelf sediment dispersal mechanisms and deposition on the Waiapu River shelf, New Zealand. Ph.D Dissertation. College of William and Mary. 283 pages.

Kniskern, T.A., Harris, C.K., Kuehl, S.A., 2006. Sediment Deposition on the Waiapu River Shelf, N.Z., Implication for Sediment Transport Mechanisms and Event Preservation. Ocean Sciences Meeting, Honolulu, Hawaii. Abstract OS11L-04.

Kniskern, T.A., Harris, C.K., Kuehl, S.A., 2008. Hydrodynamic, fluvial, and tectonic controls on sediment dispersal and deposition on the Waiapu River shelf, New Zealand. Ocean Sciences 2008 Meeting, Orlando, Florida. Abstract: 134, 1310.

Kuehl, S.A., Nittrouer, C.A., Allison, M.A., Faria, L.E.C., Dukat, D.A., Jaeger, J.M., Pacioni, T.D., Figueiriedo, A.G., Underkoffler, E.C., 1996. Sediment deposition, accumulation, and seabed dynamics in an energetic fine-grained coastal environment. Cont. Shelf Res. 16, 787–815.

Kuehl, S.A., Brunskill, G.J., Burnes, K., Fugate, D., Kniskern, T., Meneghini, L., 2004. Nature of sediment dispersal off the Sepik River, Papua New Guinea: preliminary sediment budget and implications for margin processes. Cont. Shelf Res. 24, 2417–2429.

Leithold, E.L., Hope, R.S., 1999. Deposition and modification of a flood layer on the northern California shelf: lessons from and about the fate of terrestrial particulate organic carbon. Mar. Geol. 154, 183–195.

Leithold, E.L., Blair, N.E., 2001. Watershed control on the carbon loading of marine sedimentary particles. Geochim. Cosmochim. Acta 65, 2231–2240.

Leithold, E.L., Perkey, D.W., Blair, N.E., Creamer, T.N., 2005. Sedimentation and carbon burial on the northern California continental shelf: the signatures of land-use change. Cont. Shelf Res. 25, 349–371.

Leithold, E.L., Blair, N.E., Perkey, D.W., 2006. Geomorphic controls on the age of particulate organic carbon from small mountainous and upland rivers. Glob. Biogeochem. Cycles 20, GB3022 11 pages.

Lewis, K.B., Pettinga, J.R., 1993. The emerging, imbricate frontal wedge of the Hikurangi Margin. In: Ballance, P.F. (Ed.), South Pacific Sedimentary Basins: Sedimentary Basins of the World. Elsevier Science Publishers B.V., Amsterdam, pp. 225–250.

Lewis, K.B., Collot, J.-Y., Lallemand, S.E., 1998. The damned Hikurangi Trough: a channel-fed trench blocked by subducting seamounts and their wake avalanches (New Zealand–France GeodyNZ Project). Basin Res. 10, 441–468.

Lewis, K.B., Lallemand, S.E., Carter, L., 2004. Collapse in a Quaternary shelf basin off East Cape, New Zealand: evidence for passage of a subducted seamount inboard of the Ruatoria giant avalanche. N.Z. J. Geol. Geophys. 47, 415–429.
Lloyd, K.H., 2007. Clay mineralogy and organic carbon associations in two adjacent watersheds, New Zealand. Masters Thesis. North Carolina State University.
Ma, Y., Wright, L.D., Friedrichs, C.T., 2008. Observations of sediment transport on the continental shelf off the mouth of the Waiapu River, New Zealand: evidence for current-supported gravity flows. Cont. Shelf Res. 28, 516–532.
Miller, A.J., Kuehl, S.A., in review. Self sedimentation for a tectonically-active margin: a modern sediment budget for the Waipaoa River, New Zealand. In review, Marine Geology.
Milliman, J.D., Syvitski, J.P.M., 1992. Geomorphic/tectonic control of sediment discharge to the ocean; the importance of small mountainous rivers. J. Geol. 100, 525–544.
Milliman, J.D., Farnsworth, K.L., Albertin, C.S., 1999. Flux and fate of fluvial sediments leaving large islands in the East Indies. J. Sea Res. 41, 97–107.
Mitra, S., Dickhut, R.M., Kuehl, S.A., Kimbrough, K.L., 1999. Polycyclic aromatic hydrocarbon, (PAH) source, sediment deposition patterns, and particle geochemistry as factors influencing PAH distribution coefficients in sediments of the Elizabeth River, VA, USA. Mar. Chem. 66, 113–127.
Morehead, M.D., Syvitski, J.P., 1999. River-plume sedimentation modeling for sequence stratigraphy; application to the Eel margin, Northern California. Mar. Geol. 154, 29–41.
Mulder, T., Syvitski, J.P.M., 1995. Turbidity currents generated at river mouths during exceptional discharge to the world's oceans. J. Geol. 103, 285–299.
Mullenbach, B.L., Nittrouer, C.S., Puig, P., Orange, D.L., 2004. Sediment deposition in a modern submarine canyon: Eel Canyon, northern California. Mar. Geol. 211, 101–119.
Nittrouer, C.A., Sternberg, R.W., 1981. The formation of sedimentary strata in an allochthonous shelf environment: the Washington continental shelf. Mar. Geol. 31, 297–316.
Nittrouer, C.A., DeMaster, D.J., McKee, B.A., Cutshall, N.H., Larsen, I.L., 1984. The effect of sediment mixing on ^{210}Pb accumulation rates for the Washington continental shelf. Mar. Geol. 54, 201–221.
Ogston, A.S., Cacchione, D.A., Sternberg, R.W., Kineke, G.C., 2000. Observations of storm and river flood-driven sediment transport on the northern California continental shelf. Cont. Shelf Res. 20, 2141–2162.
Rhoads, D.C., Boesch, D.F., Zhican, T., Fengshan, X., Liqiang, H., Nilsen, K.J., 1985. Macrobenthos and sedimentary facies on the Changjiang delta platform and adjacent continental shelf, East China Sea. Cont. Shelf Res. 4, 189–213.
Sommerfield, C.K., Nittrouer, C.A., 1999. Modern accumulation rates and a sediment budget for the Eel shelf: a flood-dominated depositional environment. Mar. Geol. 154, 227–242.
Sommerfield, C.K., Wheatcroft, R.A., 2007. Late Holocene sediment accumulation on the northern California shelf: oceanic, fluvial, and anthropogenic influences. Geol. Soc. Amer. Bull. 117, 1120–1134.
Sommerfield, C.K., Nittrouer, C.A., Alexander, C.R., 1999. ^{7}Be as a tracer of flood sedimentation on the northern California continental margin. Cont. Shelf Res. 19, 335–361.
Srisuksawad, K., Porntepkasemsan, B., Nouchpramool, S., Yamkate, P., Carpenter, R., Peterson, M.L., Hamilton, T., 1997. Radionuclide activities, geochemistry, and accumulation rates in the Gulf of Thailand. Cont. Shelf Res. 17, 925–965.
Traykovski, P., Geyer, W.R., Irish, J.D., Lynch, J.F., 2000. The role of wave-induced density-driven fluid mud flows for cross-shelf transport on the Eel River continental shelf. Cont. Shelf Res. 20, 2113–2140.
Tsumune, D., Aoyama, M., Hirose, K., 2003. Numerical simulation of ^{137}Cs and $^{239,\ 240}$Pu concentrations by an ocean general circulation model. J. Environ. Radioact. 69, 61–84.
Wadman, H.M., 2008. Controls on continental shelf stratigraphy: Waiapu River, New Zealand. Ph.D Dissertation. College of William and Mary. 199 pages.
Wadman, H.M., McNinch, J.E., 2008. Stratigraphic spatial variation on the inner shelf of a high yield river, Waiapu River, New Zealand: implications for fine sediment dispersal and preservation. Cont. Shelf Res. 28, 865–886.
Walcott, R.I., 1987. Geodetic strain and the deformational history of the North Island of New Zealand during the late Cainozoic. Philos. Trans.-R. Soc. Lond. A321, 163–181.
Wheatcroft, R.A., 1990. Preservation potential of sedimentary event layers. Geology 18, 843–845.
Wheatcroft, R.A., 2006. Time-series measurements of macrobenthos abundance and sediment bioturbation intensity on a flood-dominated shelf. Prog. Ocenaogr. 71, 88–122.
Wheatcroft, R.A., Borgeld, J.C., 2000. Oceanic flood layers on the northern California margin: large-scale distribution and small-scale physical properties. Cont. Shelf Res. 20, 2163–2190.
Wheatcroft, R.A., Drake, D.E., 2003. Post-depositional alteration and preservation of sedimentary event layers on continental margins, I. The role of episodic sedimentation. Mar. Geol. 199, 123–137.
Wheatcroft, R.A., Sommerfield, C.K., 2005. River sediment flux and shelf sediment accumulation rates on the Pacific Northwest margin. Cont. Shelf Res. 25, 311:332.
Wright, L.D., Friedrichs, C.T., 2006. Gravity-driven sediment transport on continental shelves: a status report. Cont. Shelf Res. 26, 2092–2107.
Wright, L.D., Friedrichs, C.T., Kim, S.C., Scully, M.E., 2001. Effects of ambient currents and waves on gravity-driven sediment transport on continental shelves. Mar. Geol. 175, 25–45.
Wright, L.D., Friedrichs, C.T., Scully, M.E., 2002. Pulsational gravity-driven sediment transport on two energetic shelves. Cont. Shelf Res. 22, 2443–2460.
Wright, L.D., Ma, Y., Scully, M., Friedrichs, C.T., 2006. Observations of across shelf sediment transport during high energy flood events off the mouth of the Waiapu River, New Zealand. Eos Trans. AGU 87 (36) Ocean Science Meeting Supplemental, Abstract OS11L-03.